Chapter 1

Imaging in shot-geophone space

Till now, we have limited our data processing to midpoint-offset space. We have not analyzed reflection data directly in shot-geophone space. In practice this is often satisfactory. Sometimes it is not. The principal factor that drives us away from (y,h)-space into (s,g)-space is lateral velocity variation $v(x,z) \neq v(z)$. In this chapter, we will see how migration can be performed in the presence of $v(x,z)$ by going to (s,g)-space.

Unfortunately, this chapter has no prescription for finding $v(x,z)$, although we will see how the problem manifests itself even in apparently stratified regions. We will also see why, in practice, amplitudes are dangerous.

1.1 TOMOGRAPY OF REFLECTION DATA

Sometimes the earth strata lie horizontally with little irregularity. There we may hope to ignore the effects of migration. Seismic rays should fit a simple model with large reflection angles occurring at wide offsets. Such data should be ideal for the measurement of reflection coefficient as a function of angle, or for the measurement of the earth acoustic absorptivity $1/Q$. In his doctoral dissertation, Einar **Kjartansson** reported such a study. The results were so instructive that the study will be thoroughly reviewed here. I don't know to what extent the Grand Isle gas field typifies the rest of the earth, but it is an excellent place to begin learning about the meaning of shot-geophone offset.

1.1.1 The grand isle gas field: a classic bright spot

The dataset **Kjartansson** studied was a seismic line across the Grand Isle gas field, off the shore of Louisiana. The data contain several classic "bright spots" (strong reflections) on some rather flat undisturbed bedding. Of interest are the lateral variations in amplitude on reflections at a time depth of about 2.3 seconds on Figure 1.3. It is widely believed that such bright spots arise from gas-bearing sands.

Theory predicts that reflection coefficient should be a function of angle. For an anomalous physical situation like gas-saturated sands, the function should be distinctive. Evidence should be found on common-midpoint gathers like those shown in Figure 1.1. Looking at any one of these gathers you will note that the reflection strength versus offset seems to be a smooth, sensibly behaved function, apparently quite measurable. Using layered media theory, however, it was determined that only the most improbably bizarre medium could exhibit such strong variation of reflection coefficient with angle, particularly at small angles of incidence. (The reflection angle of the energy arriving at wide offset at time 2.5 seconds is not a large angle. Assuming constant velocity, $\arccos(2.3/2.6) = 28^\circ$). Compounding the puzzle, each common-midpoint gather shows a *different* smooth, sensibly behaved, measurable function. Furthermore, these midpoints are near one another, ten shot points spanning a horizontal distance of 820 feet.

1.1.2 Kjartansson's model for lateral variation in amplitude

The Grand Isle data is incomprehensible in terms of the model based on layered media theory. Kjartansson proposed an alternative model. Figure 1.2 illustrates a geometry in which rays travel in straight lines from any source to a flat horizontal reflector, and thence to the receivers. The only complications are "pods" of some material that is presumed to disturb seismic rays in some anomalous way. Initially you may imagine that the pods absorb wave energy. (In the end it will be unclear whether the disturbance results from energy focusing or absorbing).

Pod A is near the surface. The seismic survey is affected by it twice—once when the pod is traversed by the shot and once when it is traversed by the geophone. Pod C is near the reflector and encompasses a small area of it. Pod C is seen at all offsets h but only at one midpoint, y_0. The raypath depicted on the top of Figure 1.2 is one that is affected by all pods. It is at midpoint y_0 and at the widest offset $h_{\max}$. Find the raypath on the lower diagram in Figure 1.2.

Pod B is part way between A and C. The slope of affected points in the (y,h)-plane is part way between the slope of A and the slope of C.

Figure 1.3 shows a common-offset section across the gas field. The offset shown is the fifth trace from the near offset, 1070 feet from the shot point. Don't be tricked into thinking the water was deep. The first break at about .33 seconds is wide-angle propagation.

The power in each seismogram was computed in the interval from 1.5 to 3 seconds. The logarithm of the power is plotted in Figure 1.4a as a function of midpoint and offset. Notice streaks of energy slicing across the (y,h)-plane at about a 45° angle. The strongest streak crosses at exactly 45° through the near offset at shot point 170. This is a missing shot, as is clearly visible in Figure 1.3. Next, think about the gas sand described as pod C in the model. Any gas-sand effect in the data should show up as a streak across all offsets at the midpoint of the gas sand—that is, horizontally across the page. I don't see such streaks in Figure 1.4a. Careful study of the figure shows that the rest of the many clearly visible streaks cut the plane at an angle noticeably *less* than $\pm 45^\circ$. The explanation for the angle of the streaks in the figure is that they are like pod B. They are part way between the surface and the reflector. The angle

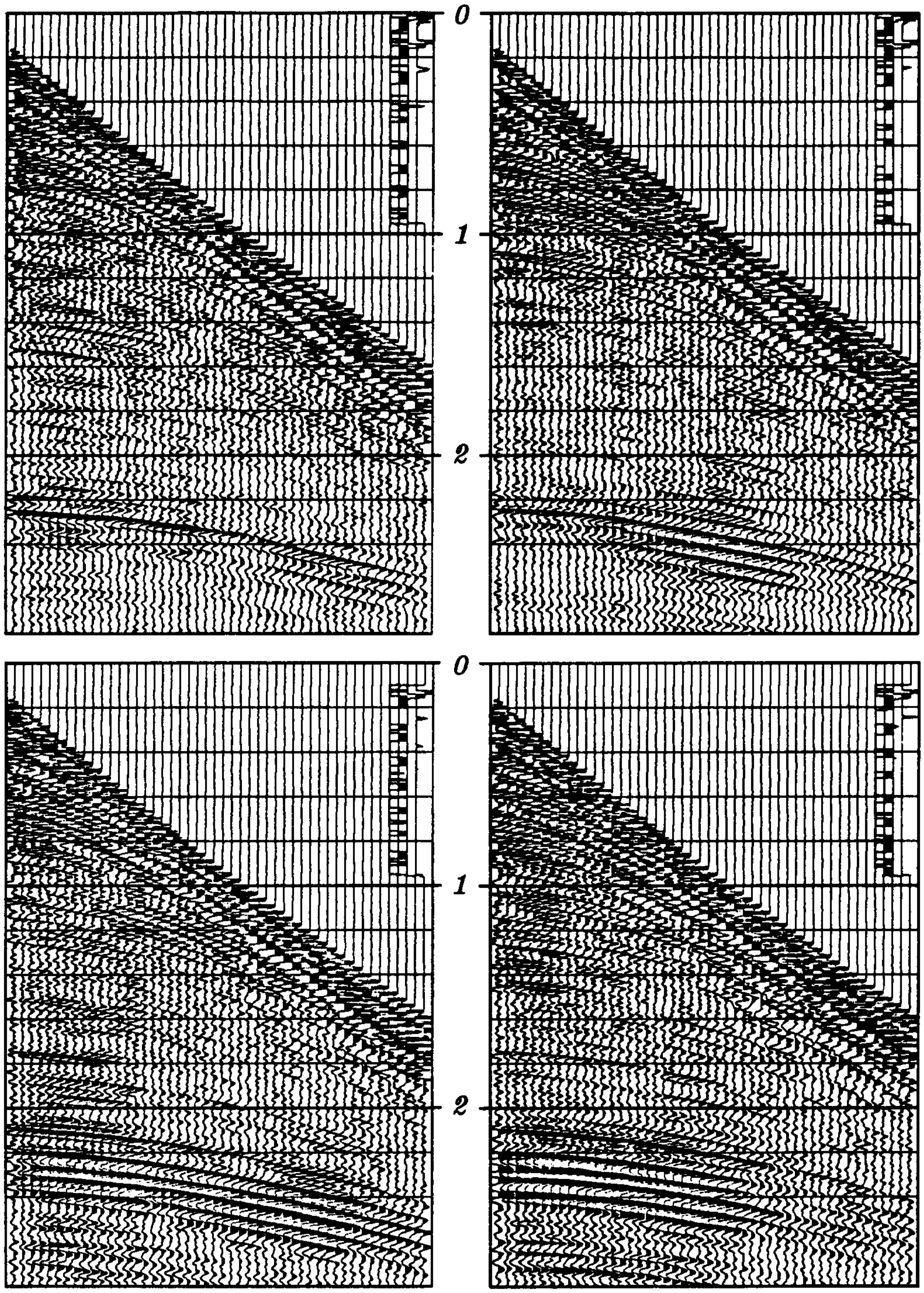

Figure 1.1: Top left is shot point 210; top right is shot point 220. No processing has been applied to the data except for a display gain proportional to time. Bottom shows shot points 305 and 315. (Kjartansson) sg-kjcmg [NR]

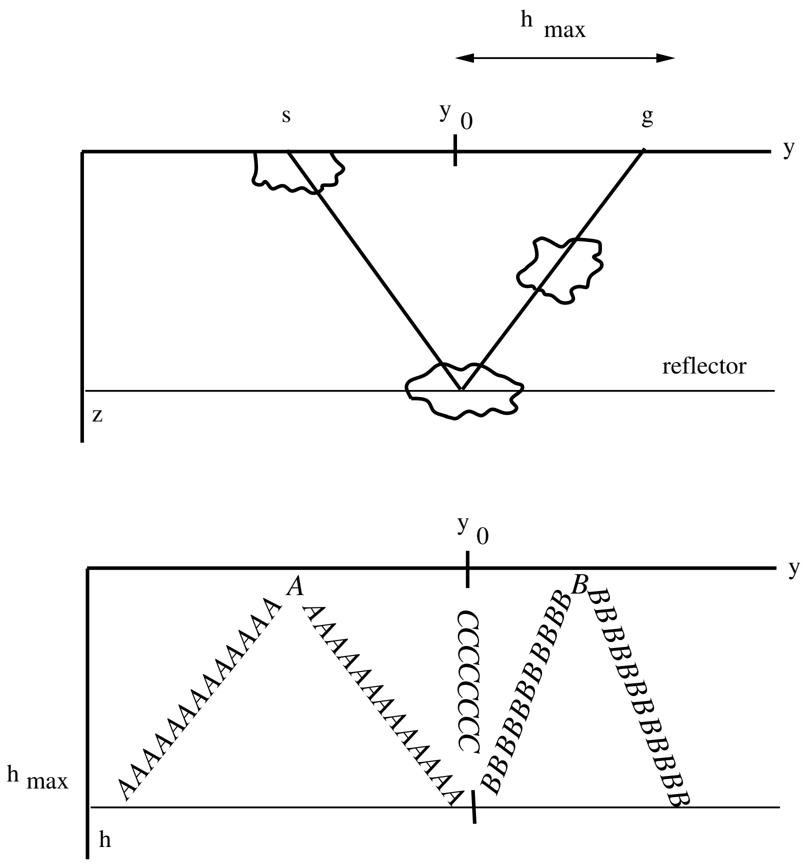

Figure 1.2: Kjartansson's model. The model on the top produces the disturbed data space sketched below it. Anomalous material in pods A, B, and C may be detected by its effect on reflections from a deeper layer. sg-kjidea [NR]

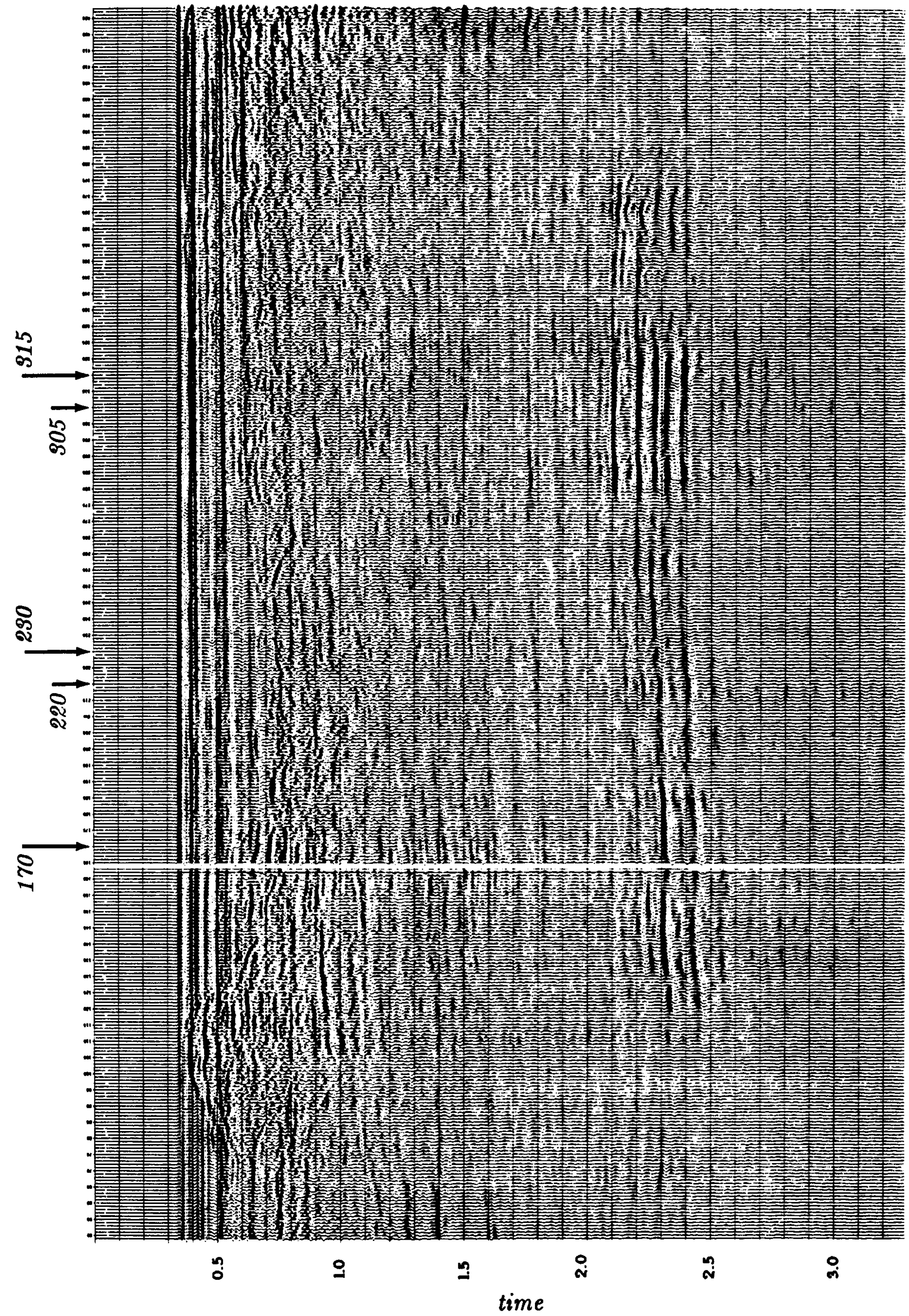

Figure 1.3: A constant-offset section across the Grand Isle gas field. The offset shown is the fifth from the near trace. (Kjartansson, Gulf) sg-kjcos [NR]

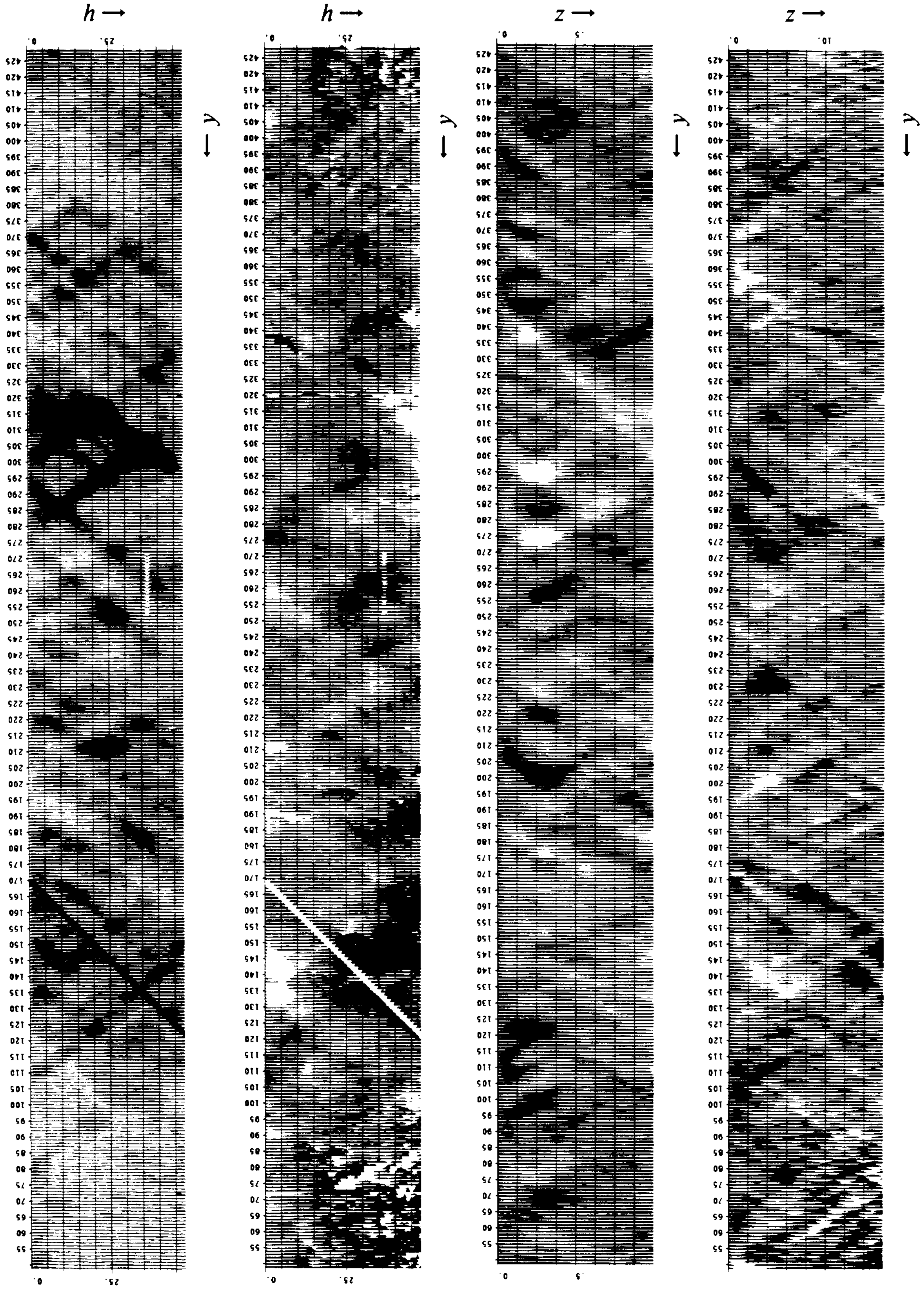

Figure 1.4: (a) amplitude (h,y), (b) timing (h,y) (c) amplitude (z,y), (d) timing (d,y) sg-kja [NR]

determines the depth. Being closer to 45° than to 0°, the pods are closer to the surface than to the reflector.

Figure 1.4b shows timing information in the same form that Figure 1.4a shows amplitude. A CDP stack was computed, and each field seismogram was compared to it. A residual time shift for each trace was determined and plotted in Figure 1.4b. The timing residuals on one of the common-midpoint gathers is shown in Figure 1.5.

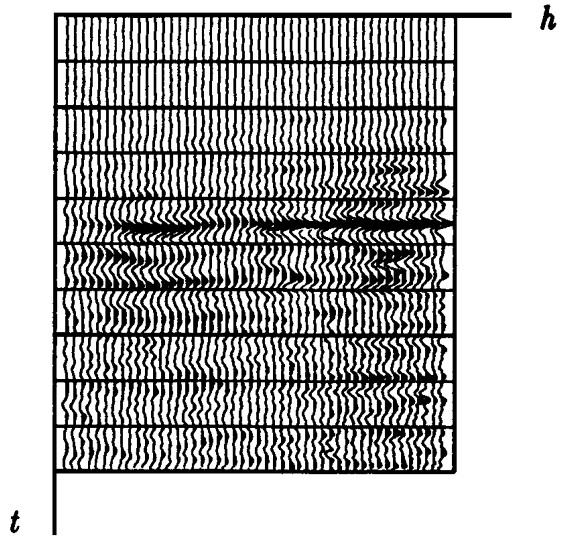

Figure 1.5: Midpoint gather 220 (same as timing of (h,y) in Figure 1.4b) after moveout. Shown is a one-second window centered at 2.3 seconds, time shifted according to an NMO for an event at 2.3 seconds, using a velocity of 7000 feet/sec. (Kjartansson) sg-kjmid [NR]

The results resemble the amplitudes, except that the results become noisy when the amplitude is low or where a "leg jump" has confounded the measurement. Figure 1.4b clearly shows that the disturbing influence on timing occurs at the same depth as that which disturbs amplitudes.

The process of *inverse* ***slant stack*** (not described in this book) enables one to determine the depth distribution of the pods. This distribution is displayed in figures 1.4c and 1.4d.

1.1.3 Rotten alligators

The sediments carried by the Mississippi River are dropped at the delta. There are sand bars, point bars, old river bows now silted in, a crow's foot of sandy distributary channels, and between channels, swampy flood plains are filled with decaying organic material. The landscape is clearly laterally variable, and eventually it will all sink of its own weight, aided by growth faults and the weight of later sedimentation. After it is buried and out of sight the lateral variations will remain as pods that will be observable by the seismologists of the future. These seismologists may see something like Figure 1.6. Figure 1.6 shows a *three-dimensional* seismic survey, that is, the ship sails many parallel lines about 70 meters apart. The top plane, a slice at constant time, shows buried river meanders.

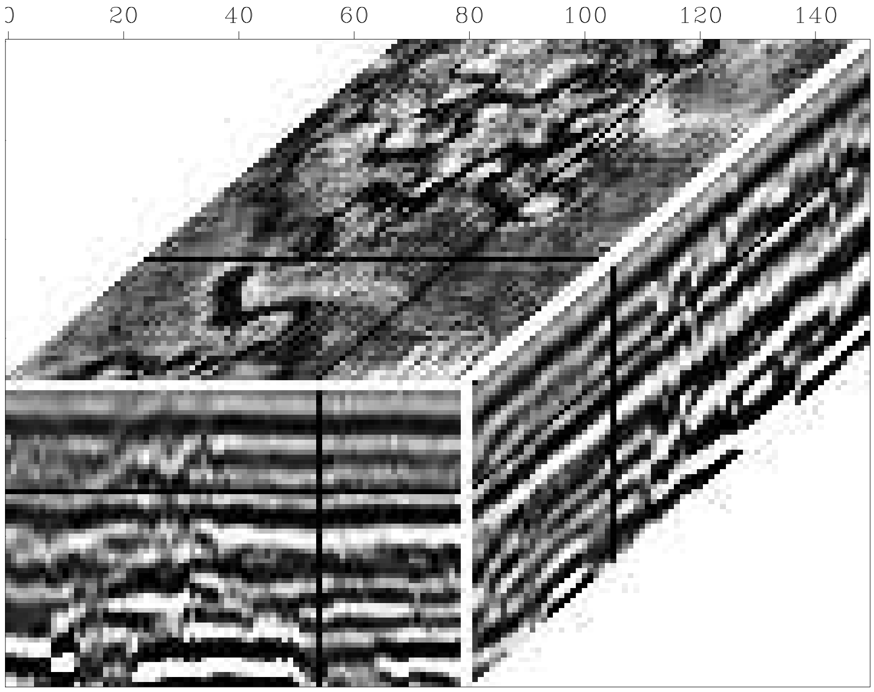

Figure 1.6: Three-dimensional seismic data from the Gulf of Thailand. Data planes from within the cube are displayed on the faces of the cube. The top plane shows ancient river meanders now submerged. (Dahm and Graebner) sg-meander [ER]

1.1.4 Focusing or absorption?

Highly absorptive rocks usually have low velocity. Behind a low velocity pod, waves should be weakened by absorption. They should also be strengthened by focusing. Which effect dominates? How does the phenomenon depend on spatial wavelength? Maybe you can figure it out knowing that black on Figure 1.4c denotes low amplitude or high absorption, and black on Figure 1.4d denotes low velocities.

I'm inclined to believe the issue is focusing, not absorption. Even with that assumption, however, a reconstruction of the velocity $v(x,z)$ for this data has never been done. This falls within the realm of "reflection **tomography**", a topic too difficult to cover here. Tomography generally reconstructs a velocity model $v(x,z)$ from travel time anomalies. It is worth noticing that with this data, however, the amplitude anomalies seem to give more reliable information.

EXERCISES:

1 Consider waves converted from pressure P waves to shear S waves. Assume an S-wave speed of about half the P-wave speed. What would Figure 1.2 look like for these waves?

1.2 SEISMIC RECIPROCITY IN PRINCIPLE AND IN PRACTICE

The principle of **reciprocity** says that the same seismogram should be recorded if the locations of the source and geophone are exchanged. A physical reason for the validity of reciprocity is that no matter how complicated a geometrical arrangement, the speed of sound along a ray is the same in either direction.

Mathematically, the reciprocity principle arises because the physical equations of elasticity are self adjoint. Thinking in terms of finite differences on a gridded earth, self-adjoint means that the matrix that translates a source anywhere to a response anywhere else is a symmetric matrix. There is a reason why such a matrix turns out to be symmetric. A product of symmetric matrices is symmetric. Running a finite difference system each time step is often a symmetric matrix, so running it many steps results in a symmetric matrix. Any actual proof is much more complicated than these few words. The final result is that very complicated electromechanical systems mixing elastic and electromagnetic waves generally fulfill the reciprocal principle. To break the reciprocal principle, you need something like a windy atmosphere so that sound going upwind has a different velocity than sound going downwind.

Anyway, since the impulse-response matrix is symmetric, elements across the matrix diagonal are equal to one another. Each element of any pair is a response to an impulsive source. The opposite element of the pair refers to an experiment where the source and receiver have had their locations interchanged.

A tricky thing about the reciprocity principle is the way antenna patterns must be handled. For example, a single vertical geophone has a natural antenna pattern. It cannot see horizontally propagating pressure waves nor vertically propagating shear waves. For reciprocity to be applicable, antenna patterns must not be interchanged when source and receiver are interchanged. The antenna pattern must be regarded as attached to the medium.

I searched our data library for split-spread land data that would illustrate reciprocity under field conditions. The constant-offset section in Figure 1.7 was recorded by vertical vibrators into vertical geophones. The survey was not intended to be a test of reciprocity, so there likely was a slight lateral offset of the source line from the receiver line. Likewise the sender and receiver arrays (clusters) may have a slightly different geometry. The earth dips in Figure 1.7 happen to be quite small although lateral velocity variation is known to be a problem in this area.

In Figure 1.8, three seismograms were plotted on top of their reciprocals. Pairs were chosen at near offset, at mid range, and at far offset. You can see that reciprocal seismograms usually have the same polarity, and often have nearly equal amplitudes. (The figure shown is the best of three such figures I prepared).

Each constant time slice in Figure 1.9 shows the reciprocity of many seismogram pairs. Midpoint runs horizontally over the same range as in Figure 1.7. Offset is vertical. Data is not recorded near the vibrators leaving a gap in the middle. To minimize irrelevant variations, moveout correction was done before making the time slices. (There is a missing source that shows up on the left side of the figure). A movie of panels like Figure 1.9 shows that the

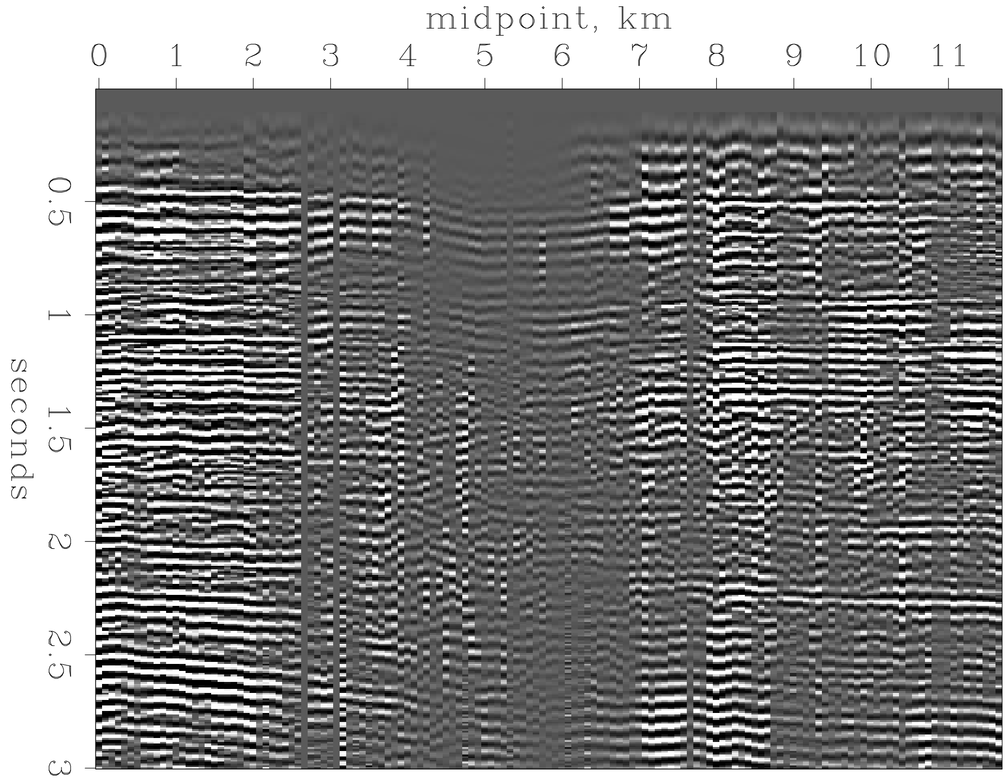

Figure 1.7: Constant-offset section from the Central Valley of California. (Chevron) sg-toldi [ER]

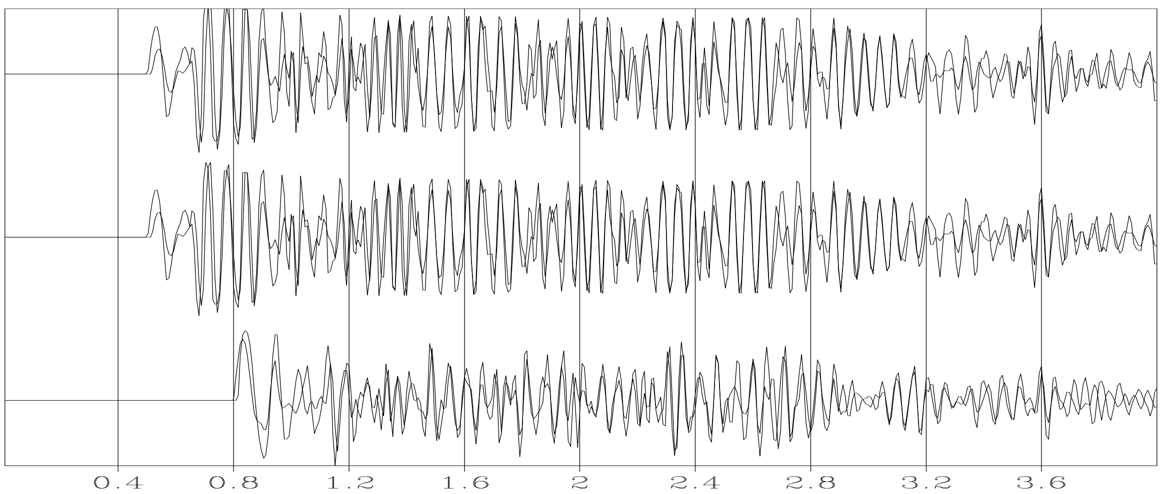

Figure 1.8: Overlain reciprocal seismograms. sg-reciptrace [ER]

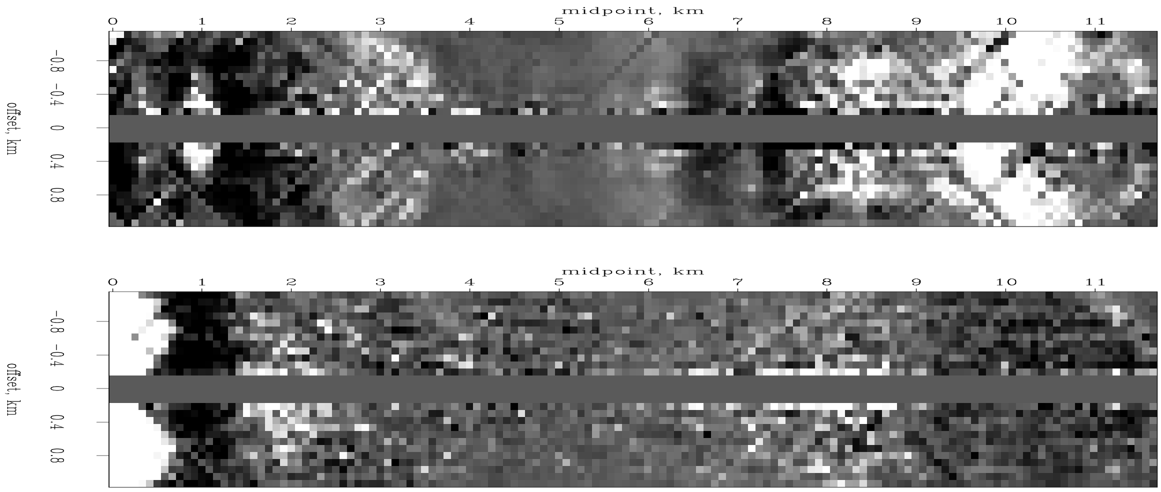

Figure 1.9: Constant time slices after NMO at 1 second and 2.5 seconds. sg-recipslice [ER]

bilateral symmetry you see in the individual panels is characteristic of all times. On these slices, you notice that the long wavelengths have the expected bilateral symmetry whereas the short wavelengths do not.

In the laboratory, reciprocity can be established to within the accuracy of measurement. This can be excellent. (See White's example in FGDP). In the field, the validity of reciprocity will be dependent on the degree that the required conditions are fulfilled. A marine air gun should be reciprocal to a hydrophone. A land-surface weight-drop source should be reciprocal to a vertical geophone. But a buried explosive shot need not be reciprocal to a surface vertical geophone because the radiation patterns are different and the positions are slightly different. Under varying field conditions Fenati and Rocca found that small positioning errors in the placement of sources and receivers can easily create discrepancies much larger than the apparent reciprocity discrepancy.

Geometrical complexity within the earth does not diminish the applicability of the principle of linearity. Likewise, geometrical complexity does not reduce the applicability of reciprocity. Reciprocity does not apply to sound waves in the presence of **wind**. Sound goes slower upwind than downwind. But this effect of wind is much less than the mundane irregularities of field work. Just the weakening of echoes with time leaves noises that are not reciprocal. Henceforth we will presume that reciprocity is generally applicable to the analysis of reflection seismic data.

1.3 SURVEY SINKING WITH THE DSR EQUATION

Exploding-reflector imaging will be replaced by a broader imaging concept, ***survey sinking***. A new equation called the double-square-root (DSR) equation will be developed to implement survey-sinking imaging. The function of the **DSR equation** is to downward continue an entire seismic survey, not just the geophones but also the shots. Peek ahead at equation (1.13) and you will see an equation with two square roots. One represents the cosine of the wave *arrival* angle. The other represents the *takeoff* angle at the shot. One cosine is expressed in terms of k_g, the Fourier component along the geophone axis of the data volume in (s,g,t)-space. The other cosine, with k_s, is the Fourier component along the shot axis.

1.3.1 The survey-sinking concept

The exploding-reflector concept has great utility because it enables us to associate the seismic waves observed at zero offset in many experiments (say 1000 shot points) with the wave of a single thought experiment, the exploding-reflector experiment. The exploding-reflector analogy has a few tolerable limitations connected with lateral velocity variations and multiple reflections, and one major limitation: it gives us no clue as to how to migrate data recorded at nonzero offset. A broader imaging concept is needed.

Start from field data where a survey line has been run along the x-axis. Assume there has been an infinite number of experiments, a single experiment consisting of placing a point source or shot at s on the x-axis and recording echoes with geophones at each possible location g on the x-axis. So the observed data is an upcoming wave that is a two-dimensional function of s and g, say $P(s,g,t)$.

Previous chapters have shown how to downward continue the *upcoming* wave. Downward continuation of the upcoming wave is really the same thing as downward continuation of the geophones. It is irrelevant for the continuation procedures where the wave originates. It could begin from an exploding reflector, or it could begin at the surface, go down, and then be reflected back upward.

To apply the imaging concept of survey sinking, it is necessary to downward continue the sources as well as the geophones. We already know how to downward continue geophones. Since reciprocity permits interchanging geophones with shots, we really know how to downward continue shots too.

Shots and geophones may be downward continued to different levels, and they may be at different levels during the process, but for the final result they are only required to be at the same level. That is, taking z_s to be the depth of the shots and z_g to be the depth of the geophones, the downward-continued survey will be required at all levels $z = z_s = z_g$.

The image of a reflector at (x,z) is defined to be the strength and polarity of the echo seen by the closest possible source-geophone pair. Taking the mathematical limit, this closest pair is a source and geophone located together on the reflector. The travel time for the echo is zero. This survey-sinking concept of imaging is summarized by

$$\text{Image}(x,z) \quad = \quad \text{Wave}(s=x, g=x, z, t=0) \tag{1.1}$$

For good quality data, i.e. data that fits the assumptions of the downward-continuation method, energy should migrate to zero offset at zero travel time. Study of the energy that doesn't do so should enable improvement of the model. Model improvement usually amounts to improving the spatial distribution of velocity.

1.3.2 Survey sinking with the double-square-root equation

An equation was derived for paraxial waves. The assumption of a *single* plane wave means that the arrival time of the wave is given by a single-valued $t(x,z)$. On a plane of constant z, such as the earth's surface, Snell's parameter p is measurable. It is

$$\frac{\partial t}{\partial x} \quad = \quad \frac{\sin\theta}{v} \quad = \quad p \tag{1.2}$$

In a borehole there is the constraint that measurements must be made at a constant x, where the relevant measurement from an *upcoming* wave would be

$$\frac{\partial t}{\partial z} \quad = \quad -\frac{\cos\theta}{v} \quad = \quad -\sqrt{\frac{1}{v^2} - \left(\frac{\partial t}{\partial x}\right)^2} \tag{1.3}$$

Recall the time-shifting partial-differential equation and its solution U as some arbitrary functional form f:

$$\frac{\partial U}{\partial z} \quad = \quad -\frac{\partial t}{\partial z}\frac{\partial U}{\partial t} \tag{1.4}$$

$$U \quad = \quad f\left(t - \int_0^z \frac{\partial t}{\partial z}\, dz\right) \tag{1.5}$$

The partial derivatives in equation (1.4) are taken to be at constant x, just as is equation (1.3). After inserting (1.3) into (1.4) we have

$$\frac{\partial U}{\partial z} \quad = \quad \sqrt{\frac{1}{v^2} - \left(\frac{\partial t}{\partial x}\right)^2}\ \frac{\partial U}{\partial t} \tag{1.6}$$

Fourier transforming the wavefield over (x,t), we replace $\partial/\partial t$ by $-i\omega$. Likewise, for the traveling wave of the Fourier kernel $\exp(-i\omega t + ik_x x)$, constant phase means that $\partial t/\partial x = k_x/\omega$. With this, (1.6) becomes

$$\frac{\partial U}{\partial z} \quad = \quad -i\omega\sqrt{\frac{1}{v^2} - \frac{k_x^2}{\omega^2}}\ U \tag{1.7}$$

The solutions to (1.7) agree with those to the scalar wave equation unless v is a function of z, in which case the scalar wave equation has both upcoming and downgoing solutions, whereas (1.7) has only upcoming solutions. We go into the lateral space domain by replacing ik_x by $\partial/\partial x$. The resulting equation is useful for superpositions of many local plane waves and for lateral velocity variations $v(x)$.

1.3.3 The DSR equation in shot-geophone space

Let the geophones descend a distance dz_g into the earth. The change of the travel time of the observed upcoming wave will be

$$\frac{\partial t}{\partial z_g} \quad = \quad -\sqrt{\frac{1}{v^2} - \left(\frac{\partial t}{\partial g}\right)^2} \tag{1.8}$$

Suppose the shots had been let off at depth dz_s instead of at $z = 0$. Likewise then,

$$\frac{\partial t}{\partial z_s} \quad = \quad - \sqrt{\frac{1}{v^2} - \left(\frac{\partial t}{\partial s}\right)^2} \tag{1.9}$$

Both (1.8) and (1.9) require minus signs because the travel time decreases as either geophones or shots move down.

Simultaneously downward project both the shots and geophones by an identical vertical amount $dz = dz_g = dz_s$. The travel-time change is the sum of (1.8) and (1.9), namely,

$$dt \quad = \quad \frac{\partial t}{\partial z_g}\, dz_g + \frac{\partial t}{\partial z_s}\, dz_s \quad = \quad \left(\frac{\partial t}{\partial z_g} + \frac{\partial t}{\partial z_s}\right) dz \tag{1.10}$$

or

$$\frac{\partial t}{\partial z} \quad = \quad - \left(\sqrt{\frac{1}{v^2} - \left(\frac{\partial t}{\partial g}\right)^2} + \sqrt{\frac{1}{v^2} - \left(\frac{\partial t}{\partial s}\right)^2}\right) \tag{1.11}$$

This expression for $\partial t/\partial z$ may be substituted into equation (1.4):

$$\frac{\partial U}{\partial z} \quad = \quad + \left(\sqrt{\frac{1}{v^2} - \left(\frac{\partial t}{\partial g}\right)^2} + \sqrt{\frac{1}{v^2} - \left(\frac{\partial t}{\partial s}\right)^2}\right) \frac{\partial U}{\partial t} \tag{1.12}$$

Three-dimensional Fourier transformation converts upcoming wave data $u(t,s,g)$ to $U(\omega,k_s,k_g)$. Expressing equation (1.12) in Fourier space gives

$$\frac{\partial U}{\partial z} \quad = \quad -i\,\omega \left[\sqrt{\frac{1}{v^2} - \left(\frac{k_g}{\omega}\right)^2} + \sqrt{\frac{1}{v^2} - \left(\frac{k_s}{\omega}\right)^2}\right] U \tag{1.13}$$

Recall the origin of the two square roots in equation (1.13). One is the cosine of the arrival angle at the geophones divided by the velocity at the geophones. The other is the cosine of the takeoff angle at the shots divided by the velocity at the shots. With the wisdom of previous chapters we know how to go into the lateral space domain by replacing ik_g by $\partial/\partial g$ and ik_s by $\partial/\partial s$. To incorporate lateral velocity variation $v(x)$, the velocity at the shot location must be distinguished from the velocity at the geophone location. Thus,

$$\boxed{\frac{\partial U}{\partial z} \quad = \quad \left[\sqrt{\left(\frac{-i\omega}{v(g)}\right)^2 - \frac{\partial^2}{\partial g^2}} + \sqrt{\left(\frac{-i\omega}{v(s)}\right)^2 - \frac{\partial^2}{\partial s^2}}\right] U \qquad (1.14)}$$

Equation (1.14) is known as the double-square-root (DSR) equation in shot-geophone space. It might be more descriptive to call it the survey-sinking equation since it pushes geophones and shots downward together. Recalling the section on splitting and full separation we realize that the two square-root operators are commutative ($v(s)$ commutes with $\partial/\partial g$), so it is completely equivalent to downward continue shots and geophones separately or together. This equation will produce waves for the rays that are found on zero-offset sections but are absent from the exploding-reflector model.

1.3.4 The DSR equation in midpoint-offset space

By converting the DSR equation to midpoint-offset space we will be able to identify the familiar zero-offset migration part along with corrections for offset. The transformation between (g,s) recording parameters and (y,h) interpretation parameters is

$$y = \frac{g+s}{2} \tag{1.15}$$

$$h = \frac{g-s}{2} \tag{1.16}$$

Travel time t may be parameterized in (g,s)-space or (y,h)-space. Differential relations for this conversion are given by the chain rule for derivatives:

$$\frac{\partial t}{\partial g} = \frac{\partial t}{\partial y}\frac{\partial y}{\partial g} + \frac{\partial t}{\partial h}\frac{\partial h}{\partial g} = \frac{1}{2}\left(\frac{\partial t}{\partial y} + \frac{\partial t}{\partial h}\right) \tag{1.17}$$

$$\frac{\partial t}{\partial s} = \frac{\partial t}{\partial y}\frac{\partial y}{\partial s} + \frac{\partial t}{\partial h}\frac{\partial h}{\partial s} = \frac{1}{2}\left(\frac{\partial t}{\partial y} - \frac{\partial t}{\partial h}\right) \tag{1.18}$$

Having seen how stepouts transform from shot-geophone space to midpoint-offset space, let us next see that spatial frequencies transform in much the same way. Clearly, data could be transformed from (s,g)-space to (y,h)-space with (1.15) and (1.16) and then Fourier transformed to (k_y,k_h)-space. The question is then, what form would the double-square-root equation (1.13) take in terms of the spatial frequencies (k_y,k_h)? Define the seismic data field in either coordinate system as

$$U(s,g) = U'(y,h) \tag{1.19}$$

This introduces a new mathematical function U' with the same physical meaning as U but, like a computer subroutine or function call, with a different subscript look-up procedure for (y,h) than for (s,g). Applying the chain rule for partial differentiation to (1.19) gives

$$\frac{\partial U}{\partial s} = \frac{\partial y}{\partial s}\frac{\partial U'}{\partial y} + \frac{\partial h}{\partial s}\frac{\partial U'}{\partial h} \tag{1.20}$$

$$\frac{\partial U}{\partial g} = \frac{\partial y}{\partial g}\frac{\partial U'}{\partial y} + \frac{\partial h}{\partial g}\frac{\partial U'}{\partial h} \tag{1.21}$$

and utilizing (1.15) and (1.16) gives

$$\frac{\partial U}{\partial s} = \frac{1}{2}\left(\frac{\partial U'}{\partial y} - \frac{\partial U'}{\partial h}\right) \tag{1.22}$$

$$\frac{\partial U}{\partial g} = \frac{1}{2}\left(\frac{\partial U'}{\partial y} + \frac{\partial U'}{\partial h}\right) \tag{1.23}$$

In Fourier transform space where $\partial/\partial x$ transforms to ik_x, equations (1.22) and (1.23), when i and $U = U'$ are cancelled, become

$$k_s = \frac{1}{2}(k_y - k_h) \tag{1.24}$$

$$k_g = \frac{1}{2}(k_y + k_h) \tag{1.25}$$

Equations (1.24) and (1.25) are Fourier representations of (1.22) and (1.23). Substituting (1.24) and (1.25) into (1.13) achieves the main purpose of this section, which is to get the double-square-root migration equation into midpoint-offset coordinates:

$$\frac{\partial}{\partial z} U \;=\; -i\,\frac{\omega}{v}\left[\sqrt{1-\left(\frac{vk_y+vk_h}{2\omega}\right)^2}+\sqrt{1-\left(\frac{vk_y-vk_h}{2\omega}\right)^2}\;\right] U \qquad (1.26)$$

Equation (1.26) is the takeoff point for many kinds of common-midpoint seismogram analyses. Some convenient definitions that simplify its appearance are

$$G \;=\; \frac{v\,k_g}{\omega} \qquad (1.27)$$

$$S \;=\; \frac{v\,k_s}{\omega} \qquad (1.28)$$

$$Y \;=\; \frac{v\,k_y}{2\,\omega} \qquad (1.29)$$

$$H \;=\; \frac{v\,k_h}{2\,\omega} \qquad (1.30)$$

The new definitions S and G are the sines of the takeoff angle and of the arrival angle of a ray. When these sines are at their limits of ± 1 they refer to the steepest possible slopes in (s,t)- or (g,t)-space. Likewise, Y may be interpreted as the dip of the data as seen on a seismic section. The quantity H refers to stepout observed on a common-midpoint gather. With these definitions (1.26) becomes slightly less cluttered:

$$\boxed{\frac{\partial}{\partial z} U \;=\; -\frac{i\omega}{v}\left(\sqrt{1-(Y+H)^2}+\sqrt{1-(Y-H)^2}\,\right) U} \qquad (1.31)$$

EXERCISES:

1 Adapt equation (1.26) to allow for a difference in velocity between the shot and the geophone.

2 Adapt equation (1.26) to allow for downgoing pressure waves and upcoming shear waves.

1.4 THE MEANING OF THE DSR EQUATION

The double-square-root equation is not easy to understand because it is an operator in a four-dimensional space, namely, (z,s,g,t). We will approach it through various applications, each of which is like a picture in a space of lower dimension. In this section lateral velocity variation will be neglected (things are bad enough already!).

One way to reduce the dimensionality of (1.14) is simply to set $H = 0$. Then the two square roots become the same, so that they can be combined to give the familiar paraxial equation:

$$\frac{dU}{dz} \quad = \quad -i\omega\,\frac{2}{v}\sqrt{1 - \frac{v^2 k_y^2}{4\omega^2}}\;U \tag{1.32}$$

In both places in equation (1.32) where the rock velocity occurs, the rock velocity is divided by 2. Recall that the rock velocity needed to be halved in order for field data to correspond to the exploding-reflector model. So whatever we did by setting $H = 0$, gave us the same migration equation we used in chapter ??. Setting $H = 0$ had the effect of making the survey-sinking concept functionally equivalent to the exploding-reflector concept.

1.4.1 Zero-dip stacking (Y = 0)

When dealing with the offset h it is common to assume that the earth is horizontally layered so that experimental results will be independent of the midpoint y. With such an earth the Fourier transform of all data over y will vanish except for $k_y = 0$, or, in other words, for $Y = 0$. The two square roots in (1.14) again become identical, and the resulting equation is once more the paraxial equation:

$$\frac{dU}{dz} \quad = \quad -i\omega\,\frac{2}{v}\sqrt{1 - \frac{v^2 k_h^2}{4\omega^2}}\;U \tag{1.33}$$

Using this equation to downward continue hyperboloids from the earth's surface, we find the hyperboloids shrinking with depth, until the correct depth where best focus occurs is reached. This is shown in Figure 1.10.

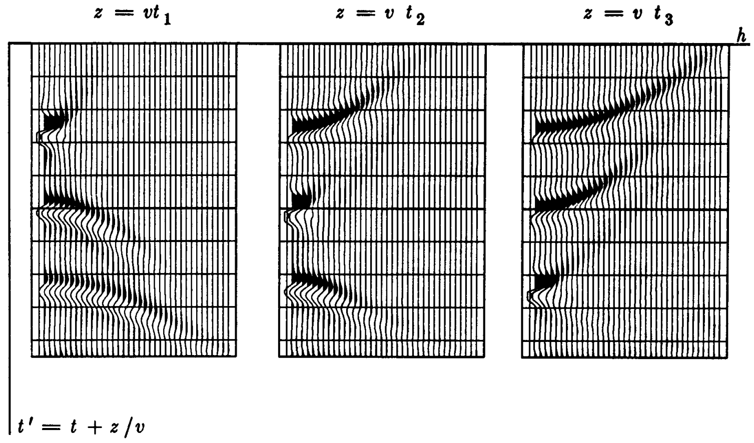

Figure 1.10: With an earth model of three layers, the common-midpoint gathers are three hyperboloids. Successive frames show downward continuation to successive depths where best focus occurs. sg-dc2 [NR]

The waves focus best at zero offset. The focus represents a downward-continued experiment, in which the downward continuation has gone just to a reflector. The reflection is strongest at zero travel time for a coincident source-receiver pair just above the reflector. Extracting the zero-offset value at $t = 0$ and abandoning the other offsets is a way of eliminating noise. (Actually it is a way of *defining* noise). Roughly it amounts to the same thing as the conventional procedure of summation along a hyperbolic trajectory on the original data. Naturally the summation can be expected to be best when the velocity used for downward continuation comes closest to the velocity of the earth. Later, offset space will be used to *determine* velocity.

1.4.2 Giving up on the DSR

The DSR operator defined by (1.14) is fun to think about, but it doesn't really go to any very popular place very easily. There is a serious problem with it. It is *not separable* into a sum of an offset operator and a midpoint operator. *Nonseparable* means that a Taylor series for (1.14) contains terms like $Y^2 H^2$. Such terms cannot be expressed as a function of Y plus a function of H. Nonseparability is a data-processing disaster. It implies that migration and stacking must be done simultaneously, not sequentially. The only way to recover pure separability would be to return to the space of S and G.

This chapter tells us that lateral velocity variation is very important. Where the velocity is known, we have the DSR equation in shot-geophone space to use for migration. A popular test data set is called the Marmousi data set. The DSR equation is particularly popular with it because with synthetic data, the velocity really is known. Estimating velocity $v(x,z)$ with real data is a more difficult task, one that is only crudely handled by by methods in this book. In fact, it is not easily done by the even best of current industrial practice.

Index